Research Square

Preprints are preliminary reports that have not undergone peer review.
They should not be considered conclusive, used to inform clinical practice,
or referenced by the media as validated information.

MAPK/NF-κB pathway modulation and oxidative stress–driven apoptosis by Solanum jabrense and solamargine in breast cancer cells

Heivila Monique da Silva Alexandre
Federal University of Paraíba
Pablo Vinícius Soares de Santana
Federal University of Paraíba
Karinne Kelly Gadelha Marques
Federal University of Paraíba
Adegildo Rolim de Abreu Júnior
Federal University of Paraíba
Ramon Ramos Marques de Souza
Federal University of Paraíba
Anauara Lima e Silva
Federal University of Paraíba
Adiel Henrique de Oliveira Pontes
Federal University of Paraíba
Sâmia Sousa Duarte
Federal University of Paraíba
Josean Fechine Tavares
Federal University of Paraíba
Maria de Fátima Agra
Federal University of Paraíba
Luciana Scotti
Federal University of Paraíba
Marcus Tullius Scotti
Federal University of Paraíba
Marianna Vieira Sobral
Federal University of Paraíba
Juan Carlos Ramos Gonçalves
juan.goncalves@academico.ufpb.br

Federal University of Paraíba

Research Article

Keywords: Cancer, S. jabrense, Alkaloids, Citotoxicity, Molecular docking

Posted Date: April 28th, 2026

DOI: https://doi.org/10.21203/rs.3.rs-9382393/v1

License: This work is licensed under a Creative Commons Attribution 4.0 International License.
Read Full License

Additional Declarations: No competing interests reported.

Abstract

Cancer is characterized by uncontrolled cell proliferation, immune evasion, and tissue invasion, ranking as the second leading cause of mortality worldwide. Breast cancer is the most prevalent type, accounting for 11.7% of newly diagnosed cases annually. *Solanum jabrense*, a plant endemic to Brazil, is rich in phytocompounds, particularly antitumor alkaloids. The antitumor potential of the hydroalcoholic extract of *S. jabrense* (ESJ) and an alkaloid-enriched fraction (FSJ) was investigated against human mammary adenocarcinoma cells (MCF-7 and MDA-MB-231). FSJ activity was further evaluated using a three-dimensional spheroid model. Mechanistic analyses in MCF-7 cells included apoptosis, mitochondrial depolarization, and reactive oxygen species (ROS) generation. Solamargine, isolated from *S. jabrense*, was also investigated *in vitro* and *in silico*. Half maximal inhibitory concentration (IC_{50}) values were determined at 24, 48, and 72 h. FSJ exhibited enhanced selectivity toward tumor cells, reduced spheroid size, and inhibited cell migration. Annexin V-FITC/PI staining confirmed apoptosis induction, while the JC-1 assay indicated mitochondrial depolarization. N-acetylcysteine (NAC) pre-treatment attenuated FSJ-induced cytotoxicity, indicating ROS involvement. Solamargine showed potent cytotoxicity at 48 h (IC_{50}: 8.65 ± 0.04 μM), and molecular docking analysis revealed interactions involving mitogen-activated protein kinases (MAPKs) (ERK2, JNK1, p38α) and IKKβ. This study provides the first evidence of the antitumor activity of *S. jabrense* against human mammary adenocarcinoma cells, demonstrating apoptosis and oxidative stress involvement, likely mediated by solamargine through modulation of MAPK- and NF-κB-related signaling pathways

Introduction

Cancer is a condition characterized by genetic alterations that result in uncontrolled cell growth, immune system evasion, and invasion of surrounding tissues. According to the World Health Organization, it is the second leading cause of global mortality, representing a major public health challenge [1, 2]. Breast cancer is the most prevalent type globally and the most frequently diagnosed cancer among women, accounting for 11.6% of cases in 2022 [3]. Current therapeutic strategies include surgery, radiotherapy, immunotherapy, hormone therapy, and chemotherapy, the latter being the most commonly employed [4]. However, chemotherapy is often associated with limitations such as tumor resistance and high systemic toxicity [5].

In light of these challenges, natural products are extensively investigated as alternative therapeutic strategies [6]. Several chemotherapeutic agents have already been developed from natural compounds, including Vinblastine, Vincristine, Docetaxel, and Irinotecan [7]. Brazil holds great potential for the discovery of novel bioactive compounds, including species from the Solanaceae family [6].

The genus *Solanum* L. is particularly notable for its pharmacologically active metabolites, which include compounds with anticancer properties [8]. Among these species, *Solanum jabrense* stands out due to its restricted distribution in northeastern Brazil and its richness in secondary metabolites such as

flavonoids and alkaloids with potential anticancer activity, including solamargine, which has been shown to induce apoptosis i *in vitro* models [9].

Given the clinical impact of breast cancer and the limitations of conventional therapies, this study aimed to evaluate the antitumor activity of the hydroalcoholic extract, its alkaloid-enriched fraction, and the major compound of *Solanum jabrense* in human tumor and non-tumor cell lines.

Methods and materials

S. jabrense extraction, analysis and preparation

Aerial parts (leaves and branches) of *S. jabrense* were collected in the municipality of Matureia-PB, Brazil (SisGen # AD609FD). A portion of this material was used to produce a voucher specimen and later deposited in the Lauro Pires Xavier Herbarium (JPB) at the Federal University of Paraíba (UFPB). Fresh plant material was oven-dried at approximately 60°C for 10 days, ground into a fine powder, and 500 g of the dried material was extracted with 80% methanol (8:2 MeOH:H_2O) using an ultrasonic bath for 1 h at room temperature (~ 25°C). This procedure was performed twice. The combined supernatants (4 L) were concentrated under reduced pressure at approximately 40°C using a rotary evaporator to obtain the dry extract.

For chromatographic analysis, approximately 1 mg of the hydroalcoholic extract (MeOH:H_2O, ESJ) or alkaloid-enriched fraction (FSJ) of *S. jabrense* was dissolved in 0.5 mL of 50% acetonitrile. UHPLC analyses were performed on a Nexera X2 system (Shimadzu, Kyoto, Japan) coupled to a QTOF mass spectrometer (MicroTOF-QII; Bruker Daltonics, MA, USA) with an electrospray ionization (ESI) source. Separation was achieved on a Luna C18 column (150 × 4.6 mm, 5 µm; Phenomenex, USA) at 50°C and 350 µL/min, using acetonitrile (A) and water (B) acidified with 20 mM formic acid. The gradient consisted of 0–2 min at 15:85 (A:B), a linear increase to 95% A from 2–12 min, a 5 min hold, followed by re-equilibration to 15% A for 4 min. ESI parameters were set to 4,500 V capillary voltage, 200°C desolvation temperature, 9 mL/min gas flow, and 4 bar pressure. Mass spectra were acquired in positive mode (50–1200 Da). The QTOF operated in full scan and automatic MS/MS with top-5 data-dependent acquisition. Data were processed using Data Analysis v4.2 (Bruker Daltonics®).

Prior to experiments, 1 mg of ESJ or FSJ was dissolved in DMSO to obtain a 100 mg/mL stock solution. Solamargine (SM), previously isolated from ESJ, was stored at − 20°C protected from light as a 40 mM stock solution. Serial dilutions were freshly prepared from the stocks. The final DMSO concentration did not exceed 0.5%

Cell culture

The tumor cell lines used were MCF-7 human breast adenocarcinoma (RRID: CVCL_0031) and MDA-MB-231 triple-negative human breast adenocarcinoma (RRID: CVCL_0062), while the non-tumor cell lines

were HEK-293 (human embryonic kidney) and MCF-10A (immortalized mammary epithelial cells). All cell lines were obtained from the Rio de Janeiro Cell Bank (BCRJ, Brazil) and cultured in Dulbecco's Modified Eagle Medium (DMEM) supplemented with 10% fetal bovine serum and 1% penicillin–streptomycin at 37°C in a humidified atmosphere with 5% CO_2.

MTT assay

The cells were seeded at a density of 2 × 10^5 cells/mL (MCF-7, MDA-MB-231) or 3 × 10^5 cells/mL (HEK-293, MCF-10A). After administration of FSJ, SM, or the standard drug doxorubicin (DXR), the cells were exposed to 10 µL/well of MTT (5 mg/mL) for 4 h. Optical density was measured at 570 nm using a microplate reader [10].

Nuclear analysis by Hoechst staining

MCF-7 cells (1×10^5) were plated in 24-well plates and incubated for 24 h (37°C, 5% CO_2). Afterwards, FSJ or DXR were incubated for 48 h and the cells were collected, centrifuged (500 × g, 25°C, 5 min), resuspended in PBS, and stained with 20 µL of Hoechst 34580 (10 µg/mL) for 20 min. Cells were analyzed by laser scanning confocal microscopy (Leica, German) and fluorescence intensity was quantified using ImageJ software (NIH, USA) [11].

Assessment of cell death by AO/PI double staining

MCF-7 cells (1 × 10^5 cells/mL) were seeded in 24-well plates and incubated for 24 h (37°C, 5% CO_2), then treated with FSJ (17 or 35 µg/mL) or DXR (4 µM) for 48 h. Cells were collected, centrifuged (500 × g, 25°C, 5 min), resuspended in PBS, and stained with acridine orange and propidium iodide (AO/PI, 10 µg/mL, 1:1). Analyses were performed by laser confocal microscopy (Leica, Germany) [11].

Apoptosis analysis by annexinV/PI assay

MCF-7 cells (1 × 10^5 cells/mL) were seeded in 24-well plates and incubated for 48 h with FSJ (17 or 35 µg/mL) or DXR (4 µM). Cells were collected, centrifuged (500 × g, 20°C, 5 min), resuspended in binding buffer, and stained with annexin V-FITC for 10 min in the dark (Merck, Germany). After washing, cells were stained with PI (20 µg/mL) and analyzed by flow cytometry (10,000 events/sample) using appropriate fluorescence filters. Data from three independent experiments performed in duplicate were processed using FlowJo software (BD, USA) [12].

Determination of mitochondrial membrane potential by JC-1 staining

MCF-7 cells (1 × 10^5 cells/mL) were plated in 24-well plates. Then treated with FSJ (35 or 17 µg/mL) for 48 h. The protonophore carbonyl cyanide m-chlorophenyl hydrazone (CCCP) was used as positive

control (50 µg/mL). The cells were incubated with the JC-1 fluorescent dye for 20 min in the dark and analyzed by laser scanning confocal microscopy.

Evaluation of FSJ Cytotoxicity in the Presence or Absence of N-acetylcysteine (NAC)

The involvement of reactive oxygen species (ROS) in the cytotoxic effect of FSJ was evaluated by pre-treating MCF-7 cells with N-acetylcysteine (NAC, 10 µM) for 3 h. MCF-7 cells (1 × 10^5 cells/mL) were cultured for 24 h and then treated with FSJ (35 or 17 µg/mL) or DXR (4 µM) for 48 h. Cell viability was determined by the MTT assay, as previously described.

Evaluation of the effect of FSJ in a 3D cell culture model (spheroids)

The hanging drop technique was performed using 25 µL drops of a cell suspension (6 × 10^4 cells/mL) placed on the lids of sterile Petri dishes and incubated for 3 days to allow spheroid formation at the air–liquid interface [13]. The spheroids were then transferred to a 24-well plate and treated with 500 µL of DMEM containing FSJ (35 or 70 µg/mL). Spheroid diameter (µm) and the radius of cell migration were evaluated at 0 and 48 h after treatment. Images were acquired using an inverted microscope with a CCD camera (Zeiss, Germany) and analyzed using ImageJ software (NIH, USA).

Molecular docking

The solamargine molecule was modeled using MarvinSketch v.23.14 and optimized by the semi-empirical MMFF method in Spartan '14'. Crystallographic structures of four apoptosis-related targets were obtained from the Protein Data Bank (RCSB PDB) and used, along with co-crystallized ligands, to analyze the interaction of solamargine with these enzymes (Table 1).

Table 1
Targets and ligands used in molecular docking.

Target	PDB ID[a]	Resolution	Ligand
JNK1	2G01	3.50 Å	73Q
p38α MAPK	7BDO	2.70 Å	TBK
ERK2	6SLG	1.33 Å	LHZ
IKKβ	4KIK	2.83 Å	KSA_700

[a] Protein Data Bank (PDB) identifiers

Molecular docking was performed using Molegro Virtual Docker 6.0. Water molecules and cofactors were removed prior to docking. A redocking step was conducted to validate the method by calculating

RMSD, with values ≤ 2 Å considered acceptable. Simulations used default parameters, and the MolDock Score evaluated ligand poses based on internal energy, hydrogen bonding, and torsional energy. Twenty independent runs were done with the MolDock SE algorithm, retaining the five best poses. A grid of 15 Å radius and 0.30 Å resolution centered on crystallographic ligand positions was used. Poses were analyzed with Discovery Studio Visualizer

Statistical Analysis

Statistical analysis was performed using GraphPad Prism (version 8.0.2; GraphPad Software Inc., San Diego, CA, USA). Data are presented as mean ± standard error of the mean (SEM). One-way analysis of variance (ANOVA) was conducted, followed by Dunnett's and Tukey's post hoc tests (significance level: $p < 0.05$). Half-maximal inhibitory concentrations (IC_{50}) and their corresponding 95% confidence intervals (95% CI) were determined using nonlinear regression analysis.

Results

Chemical constituents of Solanum jabrense

A total of 48 compounds were identified in the crude hydroalcoholic extract (MeOH:H_2O 80:20) of *S. jabrense*, with alkaloids and glycoalkaloids, being the most abundant. Saponins, phenolic compounds, and flavonoids were also detected. Solamargine ($C_{45}H_{73}NO_{15}$, m/z 868 [M + H]+) was the predominant compound, identified by specific fragments arising from dehydration and aglycone fragmentation. Its presence was confirmed by molecular mass and isotopic pattern, and it was isolated from the alkaloid fraction of the extract, with identity validated by 1D and 2D NMR. The chemical profile of the alkaloid fraction closely resembled that of the crude extract. The compounds identified are listed in Table 2, with retention time, m/z, molecular formula, and major fragment ions.

ESJ and FSJ induce cytotoxicity in human breast cancer cells

Treatment with ESJ reduced tumor cell viability in a concentration- and time-dependent manner, whereas the non-tumorigenic HEK-293 cells showed lower sensitivity (Fig. 1). Cytotoxic effects were more pronounced at higher concentrations and after 72 h of treatment. FSJ also decreased MCF-7 cell viability in a concentration-dependent manner after 48 h (Fig. 1A), while HEK-293 and MCF-10A cells were less affected (Fig. 1B). Notably, FSJ significantly reduced MCF-7 viability at low concentrations (4 µg/mL) with no significant effect on HEK-293 cells (Fig. 1B), whereas a tenfold higher concentration (40 µg/mL) was required to significantly reduce viability in MCF-10A cells. The IC_{50} values and selectivity indices for ESJ and FSJ are presented in Table 3. In contrast, doxorubicin exhibited a low selectivity index (0.36) toward MCF-10A cells.

Table 3
IC_{50} values and SI of *Solanum jabrense* in MCF-7, MDA-MB-231, and HEK cell lines.

Cell line	IC_{50}[a]			SI[b]		
	24 h	48 h	72 h	24 h	48 h	72 h
MDA-MB-231	45.44 ± 0.09	35.64 ± 0.07	20.96 ± 0.15	2.68	2.18	2.71
MCF-7	87.03 ± 0.05	27.72 ± 0.02	23.91 ± 0.03	1.39	2.83	2.41
HEK-293	121.80 ± 0.05	78.56 ± 0.80	57.54 ± 0.06	-	-	-

[a] IC_{50}: (50% inhibitory concentration); [b] SI: Selectivity index calculated as the ratio of the IC_{50} value for the non-tumor cell line (HEK) to those for the tumor cell lines.

FSJ treatment leads to nuclear alterations

The FSJ induced nuclear alterations in breast adenocarcinoma cells (MCF-7) after 48 h, as assessed by Hoechst 34580 staining and confocal microscopy (Fig. 2A). At concentrations of 17 µg/mL and 35 µg/mL, chromatin condensation and nuclear fragmentation were observed, with a significant increase in fluorescence intensity compared with the control. Quantitative analysis showed values of 241.4 ± 26% ($p < 0.05$) for FSJ at 17 µg/mL and 538.5 ± 48.3% ($p < 0.05$) for FSJ at 35 µg/mL.

Type of cell death induced by FSJ in MCF-7 cells

Figure 2B shows images of MCF-7 cells double-stained with acridine orange (AO) and propidium iodide (PI), analyzed by confocal microscopy. Treatment with FSJ significantly increased the proportion of cells in early and late apoptosis. At 35 µg/mL, early apoptosis reached 96.37 ± 6.6% and late apoptosis 1.91 ± 5.85%. At 17 µg/mL, early apoptosis was 87.54 ± 3.8% and late apoptosis 0.39 ± 0.30%. In contrast, the control group exhibited markedly lower levels, with 2.38 ± 1.86% in early apoptosis and 0.34 ± 0.2% in late apoptosis. No significant necrosis was detected in any of the analyzed groups ($p > 0.05$).

FSJ antitumoral effects in spheroids

MCF-7 spheroids incubated with FSJ for 48 h showed a significant reduction in cell migration at concentrations of 35 µg/mL (82.54 ± 4.5%) and 70 µg/mL (67.36 ± 3.13%) compared with the control group (100 ± 2.24%) ($p < 0.05$) (Fig. 2C). A significant decrease in average spheroid size was also induced by FSJ. At 70 µg/mL, spheroid size progressively decreased from 100 ± 6.9% to 87.75 ± 4.08% (0 and 48 h), whereas the control increased from 99.99 ± 3.6% to 135 ± 3.03%, highlighting the antitumor effect of FSJ.

FSJ treatment induces apoptosis

FSJ treatment significantly increased the proportion of cells in early apoptosis (Annexin V–$FITC^+/PI^-$) at concentrations of 17 µg/mL (16.2 ± 5.4%) and 35 µg/mL (68.8 ± 2.9%) ($p < 0.05$). An increase in late apoptosis/necrosis (Annexin V–$FITC^+/PI^+$) was also observed at 17 µg/mL (1.83 ± 0.47%) and 35 µg/mL

(3.78 ± 0.53%) compared with the control (early apoptosis: 0.62 ± 0.21%; late apoptosis/necrosis: 0.45 ± 0.11%; $p < 0.05$). The total percentage of apoptotic cells was significantly higher after treatment with FSJ at 17 µg/mL (18.13 ± 5.85%) and 35 µg/mL (72.65 ± 10.16%) compared with the control (1.73 ± 0.32%) ($p < 0.05$). Doxorubicin (DXR) also significantly increased the proportion of cells in early apoptosis (89.27 ± 0.26%), late apoptosis/necrosis (2.64 ± 0.15%), and total apoptosis (91.91 ± 0.38%) when compared to the control (Fig. 3A).

FSJ promotes mitochondrial depolarization

Analysis of mitochondrial potential demonstrated that FSJ treatment promoted significant depolarization of the mitochondrial membrane in MCF-7 cells marked with JC1 dye. It was evidenced an increased in the green/red fluorescence ratio (monomers/aggregates) compared with the control (Fig. 3B). This effect was more pronounced at 35 µg/mL FSJ (2.78 ± 0.15, $p < 0.05$), exceeding the positive control treated with CCCP at 50 µg/mL (1.9 ± 0.31, $p < 0.05$).

FSJ effects in MCF-7 cells is mediated by ROS

FSJ treatment (48 h) with 17 and 35 µg/mL significantly reduced MCF-7 cell viability, from 100% (control) to 59.70 ± 4.2% and 48.89 ± 2.6%, respectively ($p < 0.05$). Pretreatment with N-acetylcysteine (NAC, 10 mM) for 3 h prevented this effect, increasing viability to 168.69 ± 0.05% (17 µg/mL) and 161.7 ± 0.06% (35 µg/mL). Simillarly, doxorubicin (DXR) cytotoxicity was prevented by NAC (Fig. 3C).

Effects of solamargine from S. jabrense in MCF-7 cells

Cell viability was assessed after treatment with solamargine at concentrations ranging from 1.56 to 100 µM, resulting in an IC_{50} of 8.65 ± 0.04 µM. A concentration-dependent reduction in viability was observed in MCF-7 cells, starting at the lowest tested concentration (1.56 µM, 83.78 ± 0.03%) and becoming more pronounced at the highest concentration (100 µM, 4.5 ± 0.00%) (Fig. 4A).

Molecular interactions of solamargine with ERK2, JNK1, p38α MAPK, and IKKβ

Molecular docking analysis revealed that solamargine forms significant hydrogen bonds and π-alkyl hydrophobic interactions with ERK2, JNK1, p38α MAPK, and IKKβ. Solamargine established multiple interactions with specific residues in each target. In ERK2, notable interactions were observed with Arg413, Ser411, and Trp420; in JNK1, key interactions occurred with Asp112, Met108, and Val40, the latter being critical for inhibition. For p38α, interactions with Asp168 and Arg67, located in the active site, suggest an inhibitory role. In IKKβ, interactions with Asp103 and Lys44 (associated with NF-κB pathway inhibition) were evident (Fig. 4B). Overall, the results indicate that solamargine forms more stable interactions with JNK1 and p38α, highlighting its potential inhibitory effect on these kinases.

Discussion

The Solanaceae family is among the most extensively studied plant families, with approximately 670 identified alkaloids, including glycoalkaloids, which have been reported to exhibit diverse biological activities, such as cytotoxic effects against cancer cells [8]. The genus *Solanum* L., the largest within this family, comprises more than two thousand species of plants notable for their diversity of bioactive metabolites and pharmacological activities [8]. The species *Solanum jabrense* Agra & M. Nee is distinguished by several unique characteristics. Notably, *S. jabrense* is restricted to the northeastern region of Brazil, where it occurs specifically in high-altitude areas [9] Moreover, *S. jabrense* is rich in secondary metabolites, including flavonoids and steroidal alkaloids, with reported pharmacological properties such as anti-inflammatory and anticancer activities [8, 14]. Despite these features, relatively few studies have sought to characterize the antitumor potential of *S. jabrense*.

In the present study, ultra-performance liquid chromatography (UPLC) analysis identified 47 compounds in the crude hydroalcoholic extract of *S. jabrense* (ESJ), with alkaloids, particularly glycoalkaloids, emerging as the predominant constituents, along with saponins, phenolic compounds, and flavonoids. Our findings corroborate the chemical profile typically described for the *Solanum* genus [8, 15, 16].

Breast cancer is the most commonly diagnosed cancer and the leading cause of cancer death in women [17]. Although antineoplastic chemotherapy is widely used in breast cancer treatment, its low selectivity leads to significant side effects by damaging rapidly proliferating healthy cells, underscoring the urgent need for novel therapeutic approaches [18].

In this context, we investigated the antitumor potential of *S. jabrense* against different human breast cancer cell lines, including MCF-7 and MDA-MB-231. Human non-tumor breast epithelial cells (MCF-10A) and the HEK-293 cell line were used in the selectivity assays. Our results demonstrated that the hydroalcoholic extract (ESJ) exhibited higher selectivity toward MCF-7 mammary adenocarcinoma cells after 48 h of incubation. FSJ demonstrated markedly higher selectivity, being 15-fold more selective for tumor cells compared with the HEK-293 cell line and approximately fivefold relative to MCF-10A cells. In contrast, doxorubicin exhibited poor tumoral selectivity, which may account for the adverse effects frequently associated with this chemotherapeutic agent [19].

The effect of FSJ was subsequently evaluated using a three-dimensional (3D) cell culture model, which more accurately reproduces the *in vivo* tumor microenvironment and overcomes the limitations of traditional two-dimensional (2D) models [13]. The spheroid model allows for a more precise understanding of cell–cell interactions, treatment resistance, and the efficacy of novel therapeutic agentes. Based on the results obtained, treatment with FSJ significantly reduced cell migration and spheroid size in MCF-7 cells after 48 h, indicating its impact on tumor progression. These findings are consistent with those reported for other species of the *Solanum* genus [20].

Apoptosis is a programmed cell death process characterized by cell shrinkage, DNA fragmentation, and the formation of apoptotic bodies. Its dysregulation contributes to cancer development, making apoptosis induction a central target in antitumor therapies [21]. The antitumor effects of natural

products and their derivatives can be investigated through mechanisms such as apoptosis induction, regulation of oxidative stress, and other cellular events [11].

Treatment with FSJ significantly increased the percentage of apoptotic cells. Hoechst-stained MCF-7 cells exhibited increased fluorescence following FSJ treatment (17 and 35 µg/mL), indicating chromatin condensation and nuclear fragmentation, which are classical hallmarks of apoptosis. In addition, at the same concentrations, FSJ induced cellular alterations in AO/PI-stained MCF-7 cells, including membrane blebbing and DNA fragmentation, suggesting that apoptosis is involved in the cell death mechanism promoted by this natural compound. These effects are consistent with those reported for other species of the *Solanum* genus [22].

To confirm apoptosis as the underlying mechanism of the cytotoxic effects of FSJ in human breast cancer cells, phosphatidylserine exposure and membrane integrity were assessed using Annexin V-FITC/PI double staining [12]. Flow cytometry analysis confirmed that FSJ induces apoptosis in MCF-7 cells. Subsequently, the involvement of the mitochondrial pathway in this mode of cell death was investigated using the JC-1 assay in MCF-7 cells. This assay evaluates the activation of the intrinsic apoptotic pathway, which is modulated by changes in mitochondrial membrane permeability [23]. The results demonstrated a significant increase in mitochondrial depolarization in cells treated with FSJ or with the positive control CCCP. Similar findings have been reported in studies with other *Solanum* species, which also induced mitochondrial depolarization in MCF-7 and MDA-MB-231 cells in a concentration-dependent manner [24]. Despite these relevant findings, further studies are required to more comprehensively characterize the molecular apoptotic pathways underlying the antitumor effect of *S. jabrense*.

In tumor cells, elevated levels of reactive oxygen species (ROS) are associated with proliferation, metastasis, inhibition of apoptosis, and angiogenesis [4, 22, 25], whereas excessive ROS concentrations can lead to irreversible damage and cell death [26]. To investigate this important pathway, the effect of FSJ on the redox status of MCF-7 cells was assessed through pretreatment with an antioxidant agent. It was demonstrated that N-acetylcysteine (NAC) significantly reduced FSJ cytotoxicity, indicating the involvement of ROS in the antitumor effect of *S. jabrense*.

Solamargine, a glycoalkaloid present in several *Solanum* species as a major active compound, has been reported to exert anticancer effects against lung cancer, hepatocellular carcinoma, and prostate cancer [27]. Although its mechanisms of action, particularly in human breast cancer cells, remain incompletely understood, this study demonstrates for the first time that solamargine isolated from *S. jabrense* exhibits significant cytotoxic activity against MCF-7 cells. These findings may explain the effects attributed to ESJ and FSJ in the present study.

Mitogen-activated protein kinases (MAPKs) regulate cell proliferation and play a dual role in cancer [28]. JNK exerts antitumor functions, and natural compounds such as WZ35 induce cell death through this pathway [29, 30]. p38 MAPK, particularly the p38α isoform, is associated with cell survival and chemoresistance and also influences angiogenesis [16, 31]. The ERK pathway is also important in

tumorigenesis [32]. In addition, transcription factors such as NF-κB and the IKKβ activation pathway are central regulators of gene expression in cancer and are essential for cell proliferation and survival [33].

To further investigate the mechanisms underlying solamargine activity, *in silico* analyses were performed to evaluate potential interactions between this alkaloid and proteins involved in tumorigenesis, including MAPKs and IKKβ. Molecular docking results indicated that solamargine binds to ERK2 at residues Met108 and Lys54, suggesting possible inhibition of this pathway [32]. The alkaloid also interacts with JNK1 at residues Asp112, Asn114, and Lys153, supporting this protein as a likely molecular target of FSJ activity. Moreover, solamargine interacts with key residues of p38α (Asp168 and Ile84) in a manner comparable to known antitumor inhibitors [34] suggesting that its inhibition may attenuate tumor resistance [35]. Finally, solamargine interacts with IKKβ residues (Ile165, Asp166, and Tyr98), similarly to the inhibitor ursolic acid, highlighting its potential as a modulator of this pathway [32].

Evidence indicates that elevated reactive oxygen species (ROS) levels can induce cytotoxicity by activating or inhibiting intracellular signaling pathways, including MAPK [36] and NF-κB [37]. Taken together, the results of this study highlight the antitumor effect of *S. jabrense* in human breast cancer cells, with solamargine emerging as the most likely bioactive molecule responsible for these effects and as a modulator of key pathways involved in tumor progression, reinforcing its therapeutic potential.

Conclusion

The hydroalcoholic extract of *Solanum jabrense* (ESJ) exhibited *in vitro* antitumor activity, showing selective cytotoxicity toward MCF-7 cells compared with HEK-293 cells. The alkaloid fraction (FSJ) displayed concentration-dependent cytotoxicity and was more selective for tumor cells (MCF-7) than for non-tumor cells (HEK-293 and MCF-10A). FSJ also demonstrated antimigratory effects in MCF-7 spheroids and induced apoptosis through increased production of reactive oxygen species (ROS), generating oxidative stress. Solamargine, an alkaloid isolated from *S. jabrense*, showed cytotoxic activity and favorable interactions with key apoptotic pathway proteins, including ERK2, JNK1, p38α MAPK, and IKKβ, as revealed by molecular docking analysis. This study provides the first evidence of the antitumor potential of *S. jabrense* against human mammary adenocarcinoma cells and its ability to induce apoptosis and oxidative stress, likely through its constituent solamargine via modulation of the MAPK/NF-κB signaling pathways.

Declarations

CRediT authorship contribution statement

Alexandre, H.M.S; Santana, P.V.S.; Marques, K.K.G.; Abreu-Junior, A.R.; Sousa, R.R.M.; Silva, A.L.; Pontes, A.H.O. and Duarte, S.S.: Writing – original draft, Methodology, Formal analysis and Data curation. Tavares, J.F.; Agra, M.F.; Scotti, L.; Scotti, M.T. and Sobral, M.V.: Resources, Validation and Investigation. Gonçalves, J.C.R.: Writing – review & editing, Validation, Supervision, Resources and Conceptualization.

Declaration of competing interest

The authors declare that they have no competing interests to disclosure.

Data Availability Statement

The data that support the findings of this study are available from the corresponding author upon reasonable request.

Acknowledgments

The authors acknowledge the Brazilian funding agencies CNPq (Conselho Nacional de Desenvolvimento Científico e Tecnológico) for support through the Chamada Universal/CNPq 10/2023 (project 403382/2023-8), and CAPES (Coordenação de Aperfeiçoamento de Pessoal de Nível Superior) for providing postgraduate fellowships (2023–2024). They also thank the Fundação de Apoio à Pesquisa do Estado da Paraíba (FAPESQ-PB, Finance Code 013/2018) for essential financial support.

References

1. Allemani C et al (2018) Global surveillance of trends in cancer survival 2000-14 (CONCORD-3): analysis of individual records for 37 513 025 patients diagnosed with one of 18 cancers from 322 population-based registries in 71 countries. Lancet 391(10125):1023–1075
2. Hanahan D (2022) Hallmarks of Cancer: New Dimensions. Cancer Discov 12(1):31–46
3. Bray F et al (2024) Global cancer statistics 2022: GLOBOCAN estimates of incidence and mortality worldwide for 36 cancers in 185 countries. Cancer J Clin 74(3):229–263
4. Yang X et al (2023) Targeted therapy, immunotherapy, and chemotherapy for chordoma. Curr Med 2(1):3
5. Xie Y-H, Chen Y-X, Fang J-Y (2020) Comprehensive review of targeted therapy for colorectal cancer. Signal Transduct Target therapy 5(1):22
6. Soto KM et al (2023) Antioxidants in traditional Mexican medicine and their applications as antitumor treatments. Pharmaceuticals 16(4):482
7. Newman DJ, Cragg GM (2020) Natural products as sources of new drugs over the nearly four decades from 01/1981 to 09/2019. J Nat Prod 83(3):770–803
8. Kaunda JS, Zhang Y-J (2019) The genus solanum: an ethnopharmacological, phytochemical and biological properties review. Nat Prod bioprospecting 9(2):77–137
9. Fátima Agra M (1999) *A New Species of Solanum subgenus Leptostemonum (Solanaceae) from Chapada da Diamantina, Bahia, Brazil.* Novon, : pp. 292–295
10. Duarte SS et al (2022) Apoptotic and antioxidant effects in HCT-116 colorectal carcinoma cells by a spiro-acridine compound, AMTAC-06. Pharmacol Rep 74(3):545–554

11. Shihan MH et al (2021) A simple method for quantitating confocal fluorescent images. Biochem Biophys Rep 25:100916
12. Sousa DP et al (2023) Essential oils: Chemistry and pharmacological activities. Biomolecules 13(7):1144
13. Duval K et al (2017) Modeling physiological events in 2D vs. 3D cell culture. Physiology 32(4):266–277
14. Lima e, Silva A et al (2025) Molecular networks as strategy for dereplication of steroidal alkaloids of herbarium samples of Solanum jabrense Agra and M. Nee, an endemic and unexplored species, vol 22. Chemistry & Biodiversity, p e202402513. 6
15. Zhao Z et al (2018) Degalactotigonin, a natural compound from Solanum nigrum L., inhibits growth and metastasis of osteosarcoma through GSK3β inactivation–mediated repression of the Hedgehog/Gli1 pathway. Clin Cancer Res 24(1):130–144
16. Zhang M et al (2021) Timosaponin AIII induces G2/M arrest and apoptosis in breast cancer by activating the ATM/Chk2 and p38 MAPK signaling pathways. Front Pharmacol 11:601468
17. Sung H et al (2021) Global cancer statistics 2020: GLOBOCAN estimates of incidence and mortality worldwide for 36 cancers in 185 countries. Cancer J Clin 71(3):209–249
18. Muhamad N, Plengsuriyakarn T, Na-Bangchang K (2018) Application of active targeting nanoparticle delivery system for chemotherapeutic drugs and traditional/herbal medicines in cancer therapy: a systematic review. Int J Nanomed, : p. 3921–3935
19. Moustafa I et al (2023) Critical appraisal of clinical guidelines for prevention and management of doxorubicin-induced cardiotoxicity. J Oncol Pharm Pract 29(3):695–708
20. Ling B et al (2019) *Probing the Antitumor Mechanism of Solanum nigrum L. Aqueous Extract against Human Breast Cancer MCF7 Cells. Bioengineering.* ; 6: 112. PubMed: https://www.ncbi.nlm.nih.gov/pubmed/31835887
21. Jan R (2019) Understanding apoptosis and apoptotic pathways targeted cancer therapeutics. Adv Pharm Bull 9(2):205
22. Aziz IA (2022) Solanum Procumbens-Derived Zinc Oxide Nanoparticles Suppress Lung Cancer In Vitro through Elevation of ROS. Bioinorg Chem Appl 2022(1):2724302
23. Kumar S et al (2022) In vitro anticancer activity of methanolic extract of Justicia adhatoda leaves with special emphasis on human breast cancer cell line. Molecules 27(23):8222
24. Khan HA et al (2023) The role of mitochondrial dysfunction in cytotoxic effects of Solanum nigrum water extract on MCF-7 and MDA-MB-231 breast cancer cells. Front Bioscience-Landmark 28(8):180
25. Yang B, Chen Y, Shi J (2019) Reactive oxygen species (ROS)-based nanomedicine. Chem Rev 119(8):4881–4985
26. Kirtonia A, Sethi G, Garg M (2020) The multifaceted role of reactive oxygen species in tumorigenesis. Cell Mol Life Sci 77(22):4459–4483

27. Tai BH et al (2018) Two new steroidal alkaloid saponins from the whole plants of Solanum nigrum. Nat Prod Commun 13(11):1934578X1801301111
28. Ullah F et al (2023) Advances in the treatment of Hodgkin lymphoma: Current and future approaches. Front Oncol 13:1067289
29. Dou Y et al (2019) The Jun N-terminal kinases signaling pathway plays a seesaw role in ovarian carcinoma: A molecular aspect. J Ovarian Res 12(1):99
30. Wang L et al (2019) Curcumin derivative WZ35 inhibits tumor cell growth via ROS-YAP-JNK signaling pathway in breast cancer. J Experimental Clin Cancer Res 38(1):460
31. Lee S, Rauch J, Kolch W (2020) Targeting MAPK signaling in cancer: mechanisms of drug resistance and sensitivity. Int J Mol Sci 21(3):1102
32. Guo W et al (2020) The analysis of the anti-tumor mechanism of ursolic acid using connectively map approach in breast cancer cells line MCF-7. Cancer Manage Res, : p. 3469–3476
33. Wang Q et al (2024) Rosa roxburghii Tratt juice inhibits NF-κB and increases IL-2 to alleviates the Foxp3-mediated Tregs imbalance in the peripheral blood of arseniasis patients. Food Sci Biotechnol 33(4):935–944
34. Khan MF et al (2019) Dibenzepinones, dibenzoxepines and benzosuberones based p38α MAP kinase inhibitors: Their pharmacophore modelling, 3D-QSAR and docking studies. Comput Biol Med 110:175–185
35. Igea A, Nebreda AR (2015) The stress kinase p38α as a target for cancer therapy. Cancer Res 75(19):3997–4002
36. Li B et al (2023) Phytochemical profile and biological activities of the essential oils in the aerial part and root of Saposhnikovia divaricata. Sci Rep 13(1):8672
37. Ahmadian E et al (2017) *Anti-cancer effects of citalopram on hepatocellular carcinoma cells occur via cytochrome C release and the activation of NF-kB.* Anti-Cancer Agents in Medicinal Chemistry-Anti-Cancer Agents). 17(11):1570–1577

Table 2

Table 2 is available in the Supplementary Files section.

Figures

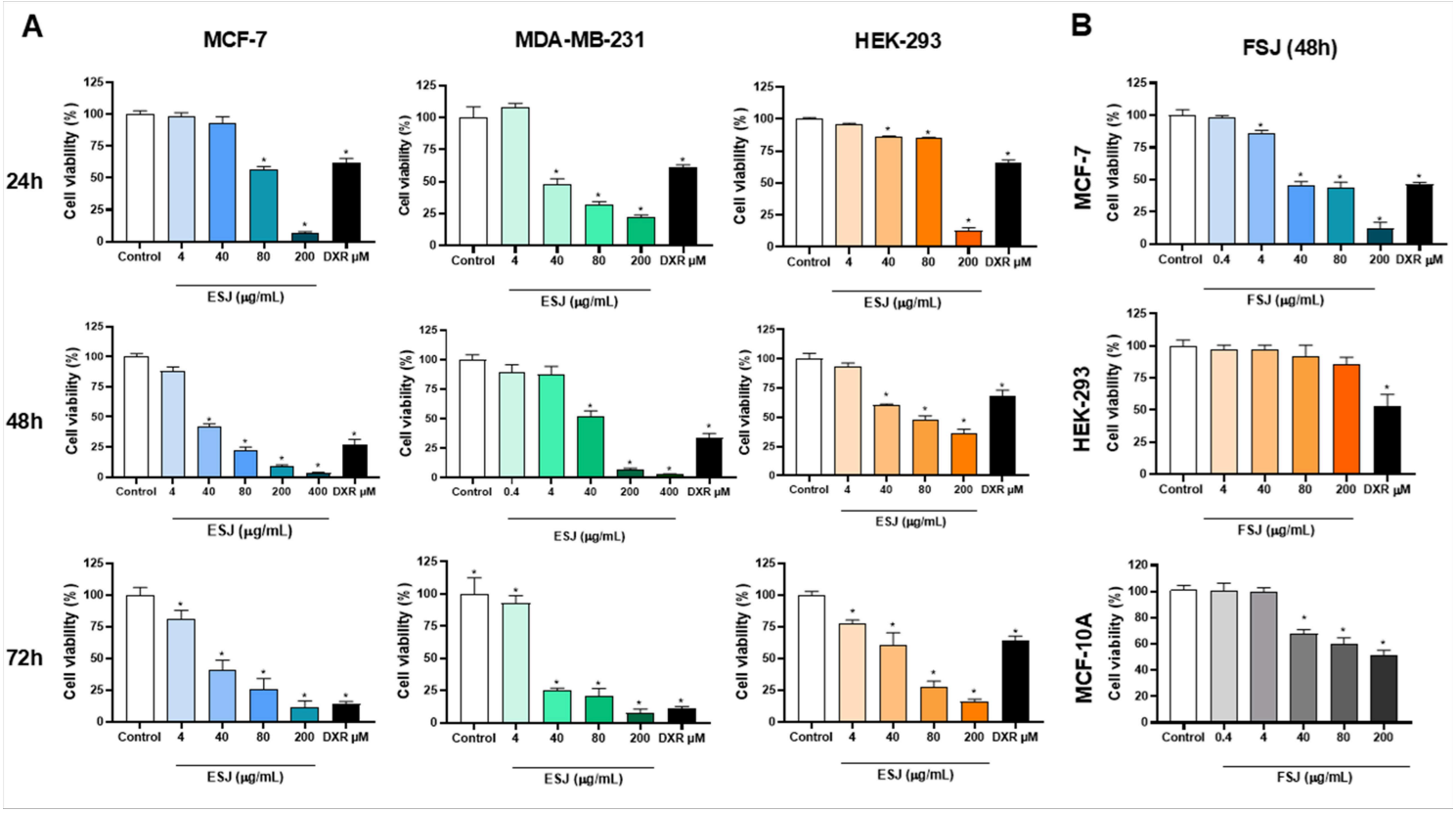


Figure 1

Cytotoxicity of ESJ and FSJ in breast adenocarcinoma cell lines and non-tumor cell lines after 24, 48, and 72 hours of treatment; **A** Cell viability for the breast adenocarcinoma cell lines MCF-7 and MDA-MB-231, as well as the non-tumor renal cell line HEK-293, after 24 h, 48 h, and 72 h of treatment with ESJ. **B** Cell viability of MCF-7, HEK-293, and the non-tumoral breast epithelial cell line MCF-10A after 48 h of treatment with FSJ. Data are expressed as mean ± SEM from three independent experiments performed in triplicate, analyzed by one-way Analysis of Variance (ANOVA), followed by Dunnett's test ($p < 0.05$). DXR: doxorubicin.

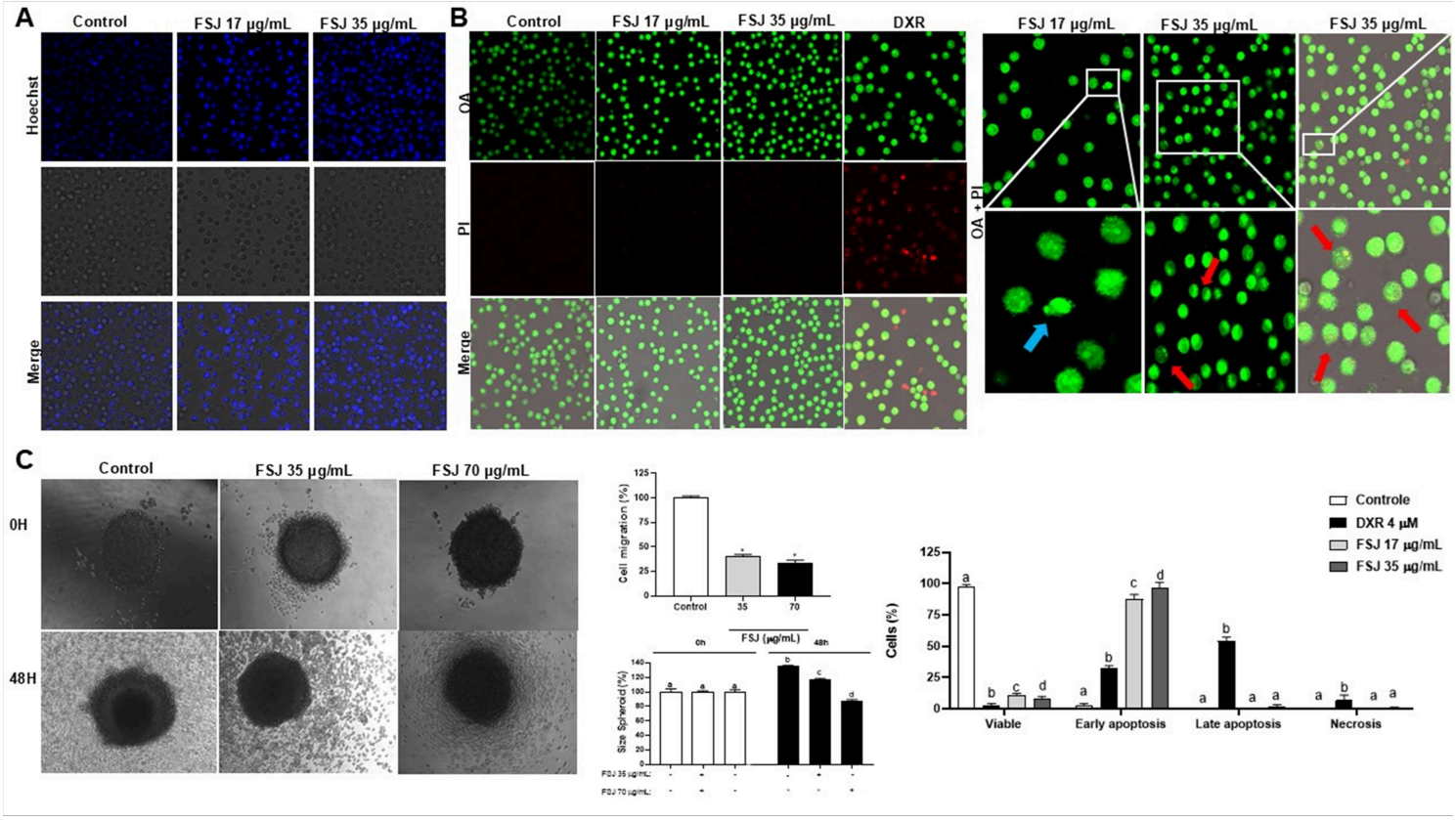


Figure 2

Antitumor effects of FSJ on MCF-7 breast adenocarcinoma cells. **A**Photomicrographs of cells stained with Hoechst 34580 after 48 h treatment with FSJ (17 and 35 µg/mL). **B** Percentage of apoptotic cells labeled with acridine orange (AO) and propidium iodide (PI) after 48 h treatment with FSJ or Doxorubicin (4 µM), observed by confocal microscopy; blue arrows indicate membrane blebs, red arrows indicate chromatin condensation and DNA fragmentation. **C**Representative images and quantification of spheroid migration and size at 0 h and after 48 h FSJ treatment. **D** Cell cycle distribution and sub-G1 percentage after 48 h FSJ treatment. Data are mean ± SEM of three independent experiments in triplicate, analyzed by ANOVA with Dunnett's or Tukey's test; different letters indicate significant differences ($p < 0.05$).

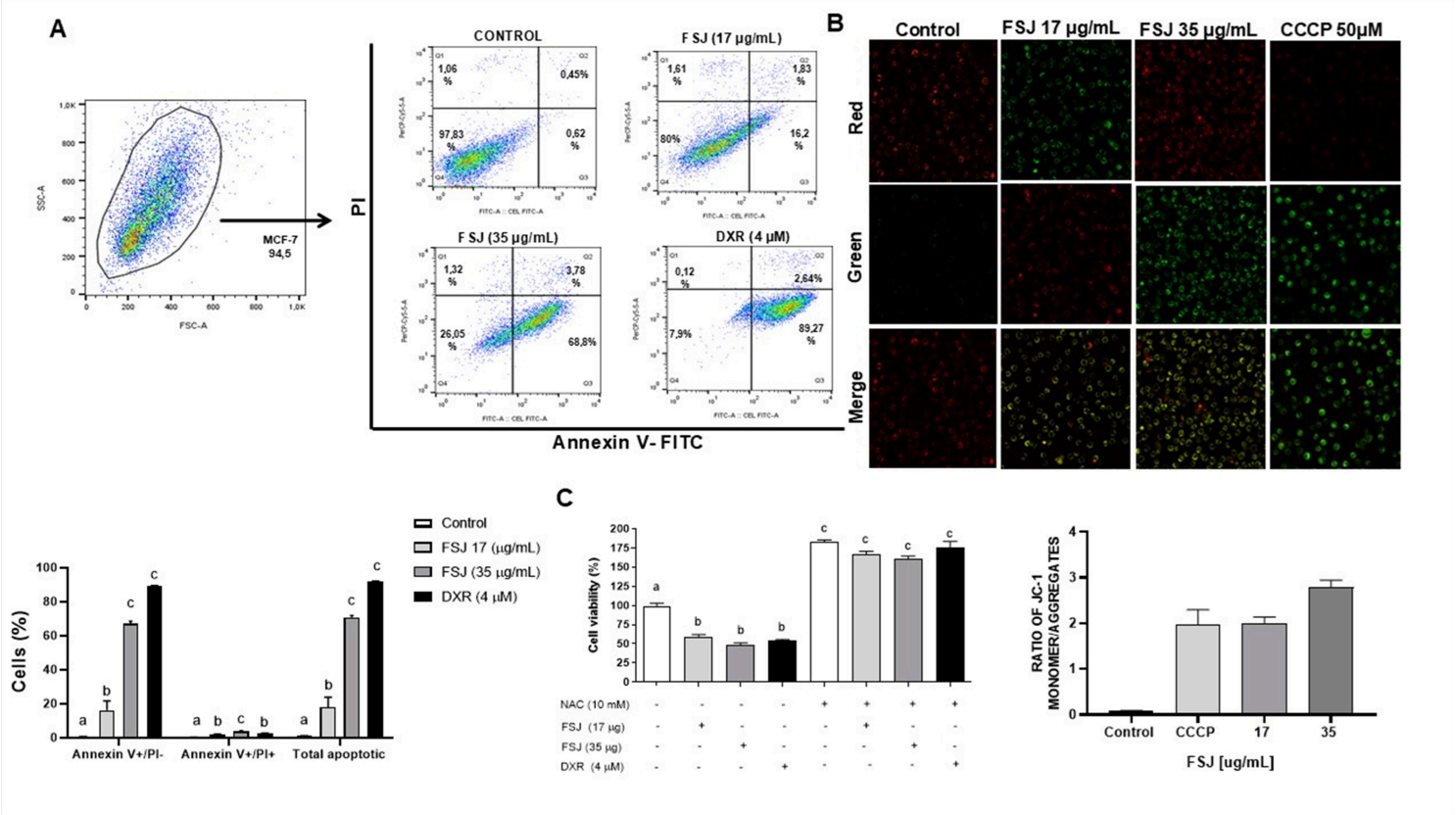


Figure 3

Antitumor effect of FSJ on MCF-7 cells**. A** Dot plots and quantification of apoptosis by flow cytometry after 48 h treatment with FSJ or doxorubicin (DXR), using Annexin V-FITC and propidium iodide (PI); 10,000 events acquired per sample. **B** Photomicrographs of MCF-7 cells stained with JC-1 after FSJ treatment; CCCP (50 µg/mL) as positive control. **C** Cell viability (%) after 48 h FSJ or DXR treatment with or without antioxidant N-acetylcysteine (NAC, 10 mM). Data represent mean ± SEM of two or three independent experiments in triplicate; analyzed by one-way ANOVA and Tukey's test. Different letters indicate significant differences ($p < 0.05$).

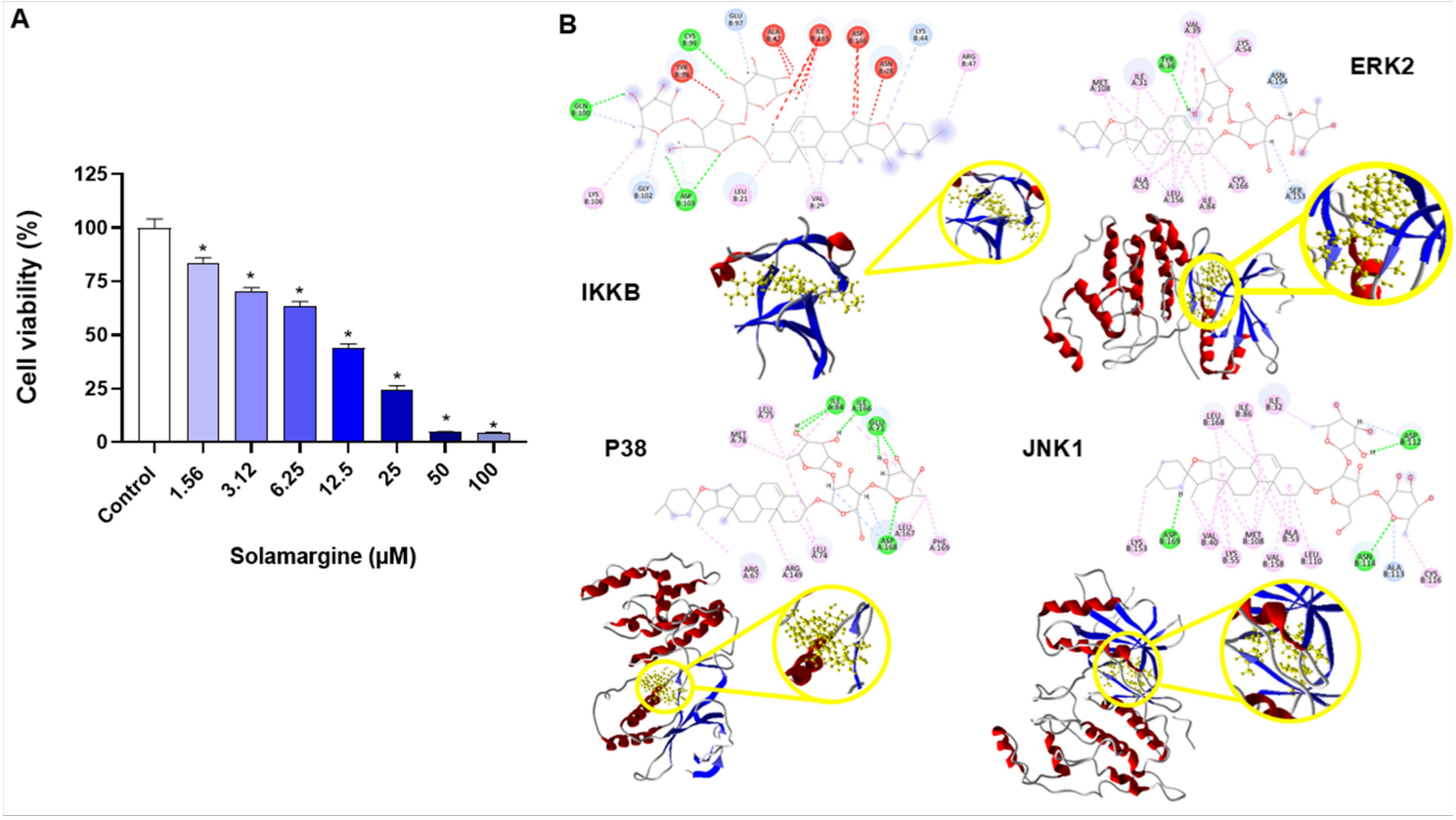


Figure 4

Cytotoxicity of Solamargine in MCF-7 Cells and Its Potential Molecular Interactions with Different Intracellular Protein Targets. (**A**) Cell viability (%) after 48 hours of Solamargine treatment. **B** 2D and 3D molecular interactions between Solamargine and the amino acid residues in the active site of the following proteins: Nuclear factor kappa B kinase subunit beta inhibitor (IKKβ) (PDB ID: 4KIK), ERK2 (Extracellular Signal-Regulated Kinase 2) (PDB ID: 6SLG), p38α MAPK (p38α Mitogen-Activated Protein Kinase) (PDB ID: 7BDO), and JNK1 (c-Jun N-terminal Kinase 1) (PDB ID: 2G01). Data are expressed as mean ± SEM from three independent experiments performed in triplicate and analyzed by one-way analysis of variance (ANOVA) followed by Dunnett's test ($p < 0.05$). Amino acid residues: Asp (aspartic acid), Glu (glutamic acid), Lys (lysine), Ile (isoleucine), Thr (threonine), Met (methionine), Cys (cysteine), Ala (alanine), Leu (leucine), Gln (glutamine), Val (valine), Asn (asparagine), Ser (serine), Tyr (tyrosine), Trp (tryptophan), His (histidine), Pro (proline), and Phe (phenylalanine)

Supplementary Files

This is a list of supplementary files associated with this preprint. Click to download.

- Table2.docx